

## Inactivation of Fecal coliforms during solar and photocatalytic disinfection by zinc oxide (ZnO) nanoparticles in compound parabolic concentrators (CPC<sub>s</sub>)

Ahmadreza Yazdanbakhsh<sup>a</sup>, Kourosch Rahmani<sup>b</sup>, Hasan Rahmani<sup>c</sup>, Mansour Sarafraz<sup>a</sup>, Masoumeh Tahmasebizadeh<sup>d</sup>, Ayat Rahmani<sup>d,\*</sup>

<sup>a</sup>Department of Environmental Health Engineering, School of Public Health, Shahid Beheshti University of Medical Sciences, Tehran, Iran.

<sup>b</sup>Department of Environmental Health Engineering, Mamasani Higher Education Complex for Health, Shiraz University of Medical Sciences, Shiraz, Iran.

<sup>c</sup>Department Environmental Health, Kashan University of Medical Sciences, Kashan, Iran.

<sup>d</sup>Research Center for Health Sciences and Technologies, Semnan University of Medical Sciences, Semnan, Iran.

Received 28 April 2018; received in revised form 5 January 2019; accepted 5 February 2019

### ABSTRACT

Water samples of 0, 50, and 100 nephelometric turbidity units (NTU) spiked with fecal coliforms (107 CFU/ml) were exposed to natural sunshine in 11 quartz glass tubes fitted with reactors' compound parabolic concentrators CPC<sub>s</sub> at two forms CPC<sub>1</sub> (with nanoparticle zinc oxide) and CPC<sub>2</sub> (without nanoparticle zinc oxide). The samples were characterized using the X-ray powder diffraction (XRD), scanning electron microscopy (SEM), and transmission electron microscope (TEM). On clear days, the complete inactivation times (more than 7-log unit reduction in bacterial population) in the systems with CPC<sub>1</sub>, and CPC<sub>2</sub> were 15, and 30 min, respectively. The maximum temperatures obtained in the water samples were 80 °C for CPC<sub>1</sub>, and 82 °C for CPC<sub>2</sub>. The use of CPC<sub>1</sub> with hydroxyl radicals (OH<sup>•</sup>) production significantly improved the efficiency of the old CPC<sub>s</sub> technique, since these systems (CPC<sub>1-2</sub>) shortened the exposure times to solar radiation and also minimized the negative effects of turbidity and also regrowth was zero in the disinfected samples. Due to two simultaneous effects of high temperatures and UV, regrowth in most ways of solar disinfection was not seen in these examples. Overall, this technology has been proved to be a good enhancement method to inactivate microorganisms under real conditions and represents a good alternative technique to drinking water treatment.

**Keywords:** Compound parabolic concentrators (CPC<sub>s</sub>), Solar disinfection, Nano photocatalyst, Fecal coliforms.

### 1. Introduction

Solar disinfection (SODIS) can significantly improve the microbiological quality of drinking water and, thus, protect the public health [1-4]. The speed of the disinfection process is a very important issue in the SODIS method; it was commonly used to disinfect water for 6 to 8 hours. One of the mechanisms of disinfection in the SODIS technique is that UV sun interferes and destroys microorganisms in the process of genetic replication of bacteria cell walls. UV<sub>A</sub> can induce cellular membrane damage through the production of reactive oxygen species [5].

Thermal inactivation is attributed to the absorption of red and infrared (IR) photons [6]. It has been reported that a temperature in the range of 12–40 °C has a negligible effect on the rate of SODIS; however, the inactivation of bacterial organisms has been observed at the temperatures greater than 45 °C. Limitations of the conventional SODIS systems have led several groups to use solar concentrators, including compound parabolic collectors (CPCs), in order to amplify spectral irradiance in solar photolytic or photocatalytic applications [7].

In recent years, advanced oxidation processes have attracted a great deal of attention thanks to their high efficiency and preventing secondary contamination, these processes are used for removing a variety of

\*Corresponding authors.

E-mail address: [ayat\\_rahmani@yahoo.com](mailto:ayat_rahmani@yahoo.com) (A. Rahmani)

biological and chemical contaminants [8-12]. Among these methods, photo catalytic removal using UV/TiO<sub>2</sub> process can remove dye compounds. The reasons of extensive use of ZnO for photocatalytic removal of contaminants in aqueous solutions include ultraviolet adsorption and its highest stability among advanced oxidation processes[8, 9, 13-16].

Photocatalysis was the acceleration of a photoreaction with the presence of the catalyst. When a semiconductor was irradiated with above band gap illumination, the radiation energy was absorbed and electrons were promoted since the valence band to the conduction band increases the formation of electron-hole pairs. If the charge carriers reach the semiconductor/water interface they may participate in redox reactions. The reactive oxygen species are very active and unique oxidants, especially the hydroxyl radical [17-19]. The reactive oxygen species can not only destroy an enormous variety of chemical contaminants in water but also cause fatal damage to microorganisms [20]. The photocatalytic properties of numerous semiconductors had been investigated (TiO<sub>2</sub>, ZnO, Fe<sub>2</sub>O<sub>3</sub>) [7, 21-27]. Between these, the most commonly used semiconductors for water treatment applications are titanium dioxide (TiO<sub>2</sub>) and zinc oxide (ZnO). TiO<sub>2</sub> and ZnO were the wide band semiconductor whose band gap energy of 3.2 and 31.3 eV corresponds to photons of the wavelength shorter than 400 nm (UV<sub>A</sub>). If the interest is solar application, active materials in the visible range are desirable [28-32].

The aim of this study is to assess the use of modified CPC mirrors to enhance the CPC<sub>s</sub> which is conventional in other works. The use of a new structure in the simultaneous use of photocatalyst and thermodynamics in disinfecting water without adding any chemicals and energy consumption is one of the main objectives of this project.

## 2. Experimental

### 2.1. Coating nanoparticles ZnO

In this study, Zinc acetate dehydrates used as the source material were dissolved in the ethanol with the concentration of 0.3 mol L<sup>-1</sup>. The blend of zinc acetate and the ethanol was heated to 80 °C in 10 min, and the ZnO thin film was corresponding to a concentration of 0.12 M. Therefore, the concentration of sol-gel obviously depended on the nature of the ZnO thin films. In this research the dip coating technique had been prepared in the laboratory. We immersed the substrate in the sol-gel solution and took it out thereafter in stable and controlled conditions to gain a film with uniform thickness. The speed of the dip coating in this test was  $V = 3.17$  cm/min and the number of coated substrate

withdrawal ranged between 5 and 8 times. The film was prepared on glass substrates annealing at 300 °C, then followed by annealing temperatures in the range of 580 °C maintaining in 60 min [33].

### 2.2. Characterization of Morphological nanoparticles

To investigate the morphology of the surface of the nanoparticles ZnO and understand immobilization of nanoparticles on the bed, SEM analysis was performed in Sharif University of Technology in Tehran. The crystal structure of the TiO<sub>2</sub> nanoparticles was also determined using the x-ray diffraction (XRD) device.

### 2.3. Preparation of Bacteria

The contaminated water sample was used for preparing the fecal coliforms. The first sampling was done by sterile containers and transferred to the laboratory. Then the culture lactose broth was used to determine the total coliforms and incubated at 35 °C for 24 h. At the next step by using a flame sterilized loop, the positive turbidity and gas in this growth were used for selecting bacteria and cultivation in the culture of EC broth (5 g nutrient broths/L of deionized water). After cultivation, the inoculated EC broth was placed in the incubator at 44 °C for 24 h [34]. The stock suspension at the stationary phase yielded bacterial concentration 10<sup>9</sup> CFU/mL. The feed suspension of the bacteria used in the reactor testing (10<sup>7</sup> CFU/mL) was produced by the dilution of 10 mL of stock into 1 L of distilled water or filtered surface water.

### 2.4. Turbidity

In our study, three turbidity levels (0, 50, and 100 NTU) were investigated and measured by a 2100 N turbid meter (HACH 2014). Turbid water samples were prepared by adding soil to distilled water. In the phase, 50 g of clay was added to 1000 ml of waters, and the prepared suspension was shaken for 60 min and left to settle for 120 min. The supernatants were collected and the turbidity was determined. Then for preparing the desired turbidity level, it was diluted with distilled water. After the preparing the desired concentration of the samples, they were sterilized by autoclaving (for 40 min at 1.0 bar) and stored at 7 °C.

### 2.5. Water sample

The tests were performed in a batch system. After preparing the samples for testing, to determine its density (number of desired bacteria) and turbidity, the samples were placed in the reactors in contact with sunlight. For evaluating the residual number of bacteria in the samples, at first, the sampling was done by a 10 mL sterile pipette in 15 min and then the samples were stored in sterile glass containers and the laboratory.

The samples were then passed through a membrane filter (0.45  $\mu\text{m}$  What-man) and then the filter was placed on the EMB agar culture medium and incubated at 35 °C for 24 h. After this time (24 h), the colony counts on the plate count method were used to determine the efficiency of disinfection [34]. Re growth counts of bacteria were determined for all experiments, by placing the samples of each reactor at room temperature for 24 and 48 h. After 24 till 48 h, the plate count method as described above was used to determine bacterial counts on the EMB agar plates. Endo agar is a selective medium, which is specific to the detection of coliforms and enteric organisms in sources such as drinking water.

### 2.6. Compound parabolic concentrator (CPC) mirrors and glass tubes

The quartz glass tubes using in the research had dimensions of 105 cm length, 3.5 cm outer diameter, 1.5 mm wall thicknesses and 1.1 L internal volume, Fig. 1S (b, c). The glass tubes can transmit 94% and 54% of UVA and UVB light, respectively. In this research, two types of the reactor CPC were used. Design of a reactor CPC was similar to the old one, with the dimensions of 30 cm width and of 100 cm lengths, the modern reactor enables more sunlight to a focal point (F), with the difference that in CPCs a black copper metal with dimensions of length, width and thickness of 100, 2.5 and 0.2 cm respectively, has been fixed vertically at the center of glass tube to absorb more light and with two flat mirrors with a 45° angle to the vertical dimension of 3 cm and a length of 100 cm were placed on both sides of the CPC to increase the light area in the reactor Fig. 1S (a). In this study we used the reflective surface of the CPCs comprising mirrors with the thickness of 1 mm; it reflects 86% of UV radiation and 96% of other types of solar radiation. The dimensions and properties of the glass tubes and each of the CPCs reactors are shown in Table 1S. Coated ZnO nanoparticles were placed at the center of the mirror (F) on the black copper metal; the performance of the reactor CPC with nanoparticles and without nanoparticles was investigated.

### 2.7. Solar experiment

All experiments were performed under natural solar radiation in Tehran-Iran, coordinates of this city are latitude: 35° 41' 39.80" N and longitude: 51° 25' 17.44" E; so, it had a very good position to use solar energy. All the experiments were conducted in duplicate on twin systems (tube + CPC) under the same meteorological conditions and to ensure reproducibility of results, each sampling was done three times. Tests started at 11 am and finished at 15 pm local time. Samples were taken after 15 to 300 min of solar exposure. As seen in

Fig. 1S (a), reactors were placed to the N-S and at an angle of 35° to 15° considering the region and the season, they were fed with samples. Solar and UV irradiances were measured with a global UV radiometer (295–385 nm UV and 400-1500 nm Solar, Model HAGNER, Sweden). The initial temperature of all samples was about 20 °C. To calculate the amount of absorbed heat energy for raising the temperature of the water, the following equation (1) is used:

$$Q = mc(T_f - T_i) \quad (1)$$

In this equation, Q (heat equivalent absorption of thermal energy) is the amount of thermal energy in J, m is the mass of water in kg, c is the heat capacity of water at the normal temperature (0 to 100 °C), the amount of c will be equal to 4190J/kg.K in the equation,  $T_i$  is the initial temperature in K,  $T_f$  is the final temperature in K.

In this research, the cumulative dose of irradiation in sunlight shining into the reactor per unit time was calculated by integrating the average solar global irradiance measured at any time during the different exposure times as shown in the following equation (2):

$$D = \int_{t_2}^{t_1} I. dt \quad (2)$$

Where D is the cumulative dose of irradiation in terms of  $\text{J/m}^2$ , I is the irradiation solar energy in terms of ( $\text{W/m}^2$ ).

## 3. Results and Discussion

### 3.1. Catalyst characterization

The photoactivity of ZnO depends on many parameters containing the crystal structure, the part between anatase and rutile phases, particle dimensions distribution, specific surface area and mean pore size. The microcrystal structure of the ZnO before and after coating was characterized with an X-ray diffractometer (XRD) analysis. XRD pattern of the pure catalyst and CDH binder catalyst coating are displayed in Fig. 1 (a, b). Results displayed in Fig. 1 (a) clearly show that there was basically no change in the X-ray diffraction pattern of ZnO [35-37]. Also, the comparison of the anatase and rutile phase before and after the nano particle coating showed that the coating process, which was carried out at 550 °C in the vacuum furnace, did not change the structure of the nanoparticle (Fig. 1 (a, b)).

The surface morphology was characterized with the scanning electron microscopy (SEM). The ZnO was located on the inner surface of the morphology of the ZnO. In Fig. 2 (a), FESEM shows the surface of the glass substrate before coating, this caused the contact of the substrate with HF and corrosion on the glass surface, leading to provide a suitable substrate for the

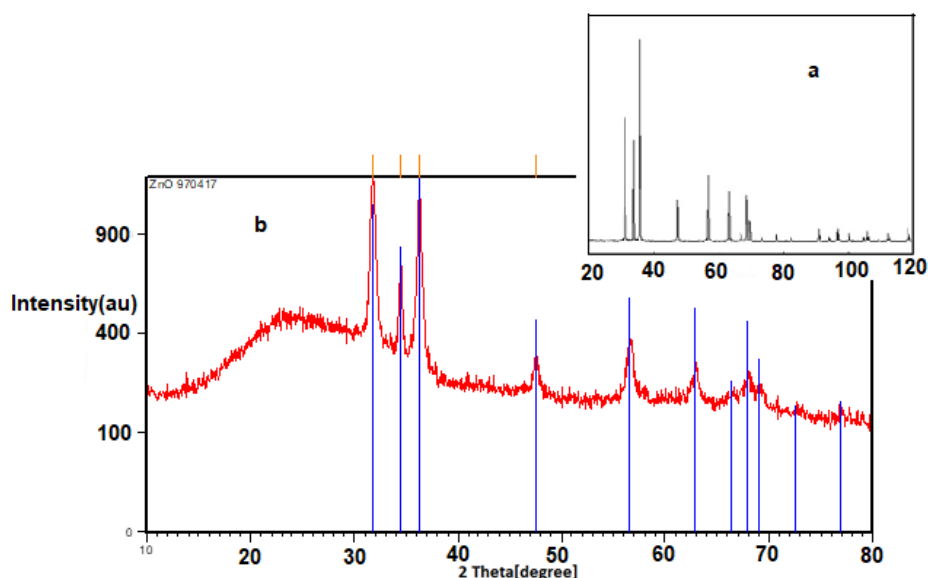


Fig. 1. XRD analysis of ZnO catalyst (a) after coating (b) before coating.

nanoparticle coating. Fig. 2 (b) shows the substrate after coating and that the nanoparticle is uniformly distributed over the entire surface. The powder ZnO had been obtained before its composition was analyzed. Fig. 2 (b) shows the size of the particles in the indicated layer. After the coating process, the size of the crystals is larger than the powdery state. Immobilization of nanoparticles and lack of change in the morphology of bed silica show the results of operation of ZnO deposition.

### 3.2. solar irradiation

The days on which the assays were carried out were sunny, with some cloud cover. Fig. 3 shows the peak sun hours of 11 to 15, so tests were done at the same time.

The maximum sunlight and UV radiations in two reactors (CPC<sub>1</sub> and CPC<sub>2</sub>) were 1298 and 39.4 W/m<sup>2</sup> respectively Fig. 3 (a, b). Another tube was kept as a controller in the dark under the same field conditions to guarantee the viability of the cells in the tube in the absence of solar radiation. The range of wavelengths of the sun's energy passes through the water, the absorption rate was low and the majority of the light passes through water [12]. In this research, to use the solar visible light wavelength in the range of 300-1600 nm, we used a black copper metal which was a strong absorbent of solar visible light. Overall, the study showed that adsorbents which were closer to absolute black body efficiently absorbed sunlight and increased the rate of temperature at F of the CPCs mirror.

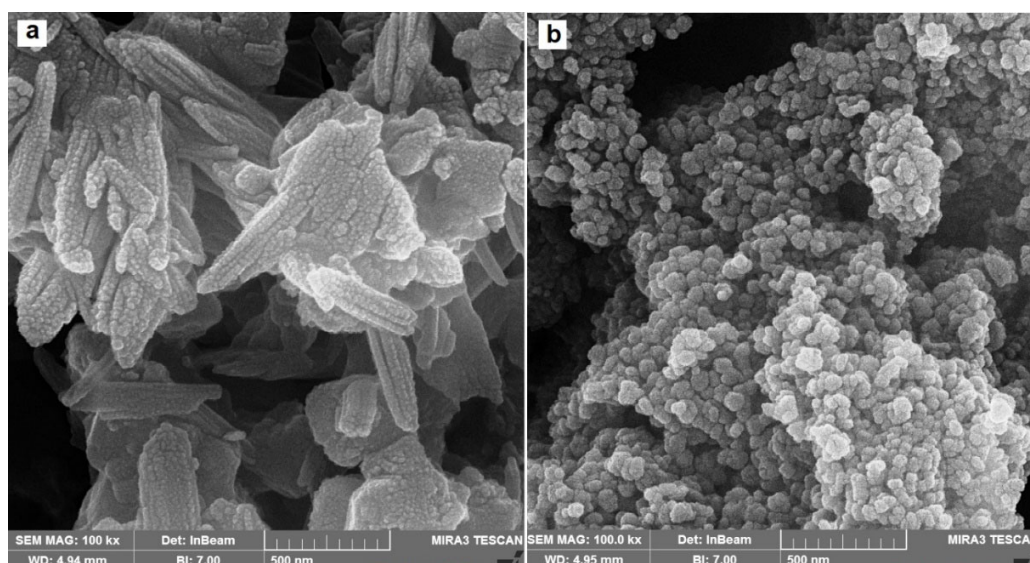
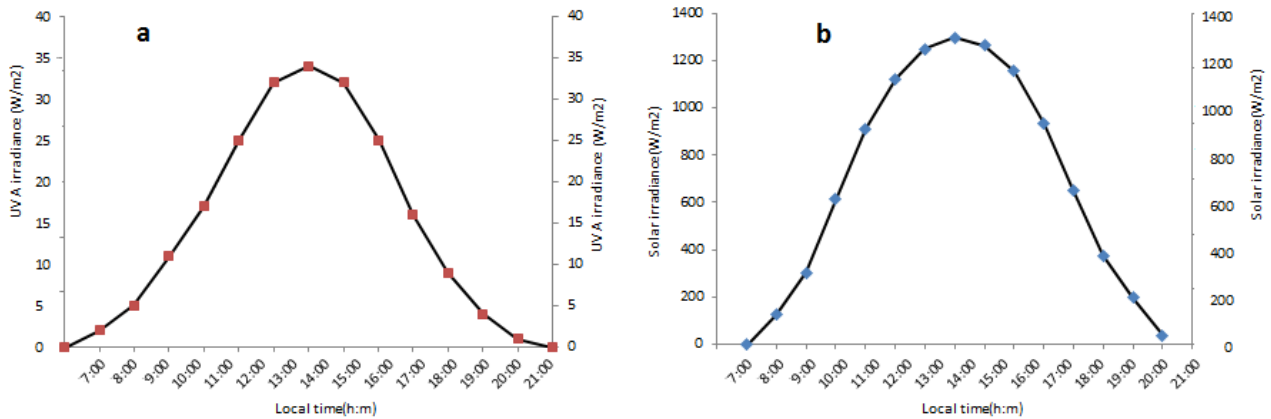


Fig. 2. FESEM image of ZnO coated glass at 500 nm (a) after coating (b) before coating.



**Fig. 3.** Graphic representations of the values of solar UV (a) and solar irradiance (b) radiations registered during the solar disinfection studies carried out the reactors CPC<sub>s</sub>.

**3.3. The effect of Catalysts on disinfection**

Fig. 5 shows inactivation of fecal coliforms in two reactors (CPC<sub>1</sub> and CPC<sub>2</sub>) with three turbidity levels (0, 50, and 100 NTU) during 4 h of exposure to natural solar irradiation. This indicates that the system with coating nanoparticle ZnO has been modified in the reactor CPC<sub>1</sub> reaching complete inactivation time at least after 15 min (0 NTU) and for the reactor CPC<sub>2</sub>, this time was than 30 min (0 NTU). An increase in solar exposure time was required to achieve bacterial inactivation in the system with the CPC<sub>2</sub> that is nearly double CPC<sub>1</sub>. In this study, coating nanoparticle ZnO has been modified in the reactor CPC<sub>1</sub> comparing to the CPC<sub>2</sub> as well as the disinfection (7 log) time was reduced to half. The inactivation of fecal coliforms using UV light can be enhanced using Advanced Oxidation Processes (AOPs). These processes involve the generation of hydroxyl radicals (OH<sup>•</sup>). AOPs have been reported as promising techniques to remove microorganisms from contaminated water. Solar driven AOPs should have lower cost and may be

applied for the sustainable treatment of drinking water and irrigation water [8-10]. With solar driven AOPs, the inactivation of fecal coliforms by UV<sub>A</sub> light is accelerated by the formation of reactive oxygen species, such as OH<sup>•</sup> radicals. Photo-induced AOPs can be divided into heterogeneous and homogeneous processes. ZnO photocatalysis is an example of a heterogeneous process and has been mostly studied for the inactivation of microorganisms. However, ZnO photocatalysis has attracted great interest due to its high efficiency for OH<sup>•</sup> generation [33, 38, 39]. Other assistances reported other responsible oxidants for inactivation such as H<sub>2</sub>O<sub>2</sub>, O<sup>•</sup>. These oxidants may cause deadly damage to microorganisms by disruption of the cell membrane and by attacking DNA and RNA. Other manners of ZnO action had been proposed including injury to the oxygen transport system within the cells and increased ion permeability in the cell membrane.

The water temperature of the systems was monitored for each sample in all the experiments (Table 1).

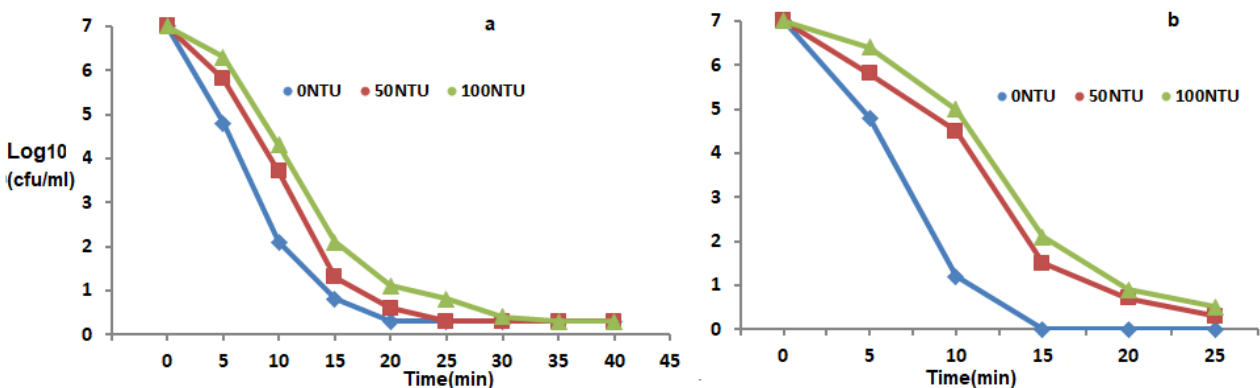


**Fig. 5.** Inactivation curves of fecal coliforms in the reactors CPC<sub>1</sub> (a), CPC<sub>2</sub> (b) during natural solar radiation exposure on clear days.

**Table 1.** Main results of the tests presented in the experimental section.

	Turbidity (NTU)	DOS (MJ/m <sup>2</sup> )	Q (kJ)	Max temperatures (°C)	Time inactivation (min)
CPC <sub>1</sub>	0	10.3	236.3	76.5	15
	50	10.7	240.6	78.9	30
	100	11.4	255.8	80.1	35
CPC <sub>2</sub>	0	11.2	249.3	79.6	30
	50	11.7	256.4	80.2	35
	100	12.2	269	82.0	35

### 3.4. The effect of solar on disinfection

The ambient temperature ranged between a minimum of 76 °C and a maximum of 82 °C. The mean temperatures registered inside the reactors fitted with CPC<sub>1</sub> and CPC<sub>2</sub> (measured every 15 min) and are shown in Fig. 6. The maximum temperatures of water samples with turbidity levels of 0, 50, and 100 NTU were 72.7, 76.6, and 78.1 °C, respectively, for CPC<sub>1</sub> (whit Nano catalyst), and 78.7, 80.2, and 82 °C, respectively, for CPC<sub>2</sub> (without Nano catalyst) Fig. 6 (a, b). All maximum temperatures were always recorded after 4 h of exposure (11:00-15:00 h, local time). Significantly higher temperatures were obtained in the most turbid water samples (100 NTU) in comparison with the other water samples (0 and 50 NTU) ( $p < 0.05$ ) for exposure periods of 4 h (CPC<sub>1</sub>) and 4 h (CPC<sub>2</sub>). As seen in Table 1, in sampling, one kg water in the reactor of CPC<sub>1</sub> received 255.2 kJ of Q (heat equivalent absorption of thermal energy) to reach the maximum temperature 80 °C, after 110 min and 11.4 MJ/m<sup>2</sup> of D (cumulative dose of energy) to reach the temperatures of 60 °C while that for CPC<sub>2</sub> to reach the maximum temperature of 82.5 °C, after the time 100 min, one kg water received 269 kJ of Q, and 12.2 MJ of D (to temperature of 62.5 °C). As previous research has

found that high temperature of 45 °C has been strong synergy between optical and thermal inactivation. A number of methods are able to enhance temperatures and accelerate the rate of thermal inactivation of organisms through the use of absorptive materials and also in these methods PET bottles were painted black in order to aid in the absorption of solar radiation [40-43]. The results in Table 1 show by placing a sunlight absorbent and receiving the radiation dose of in CPC<sub>1</sub> and CPC<sub>2</sub>, the temperature of the sample increased more than 80 °C, which is equivalent to 260 kJ of thermal energy. This change in the structure reduces the disinfection time less than 30 min. In addition to the synergistic effect of temperatures on parameters such as solar UV to increase the disinfection rate, preserving water at temperatures above 65 °C for 30 min and at 80 °C for a few seconds causes the water pasteurization, even at the presence of turbidity and organic matter. We could say that one of the most effective ways to increase the efficiency of solar disinfection methods is to enhance the efficiency of light absorption of sunlight and convert it into heat energy and use the photocatalysts. Considering the wavelengths of sunlight reaching the earth surface, the wavelength was in the maximum range of 300–1, 600 nm.

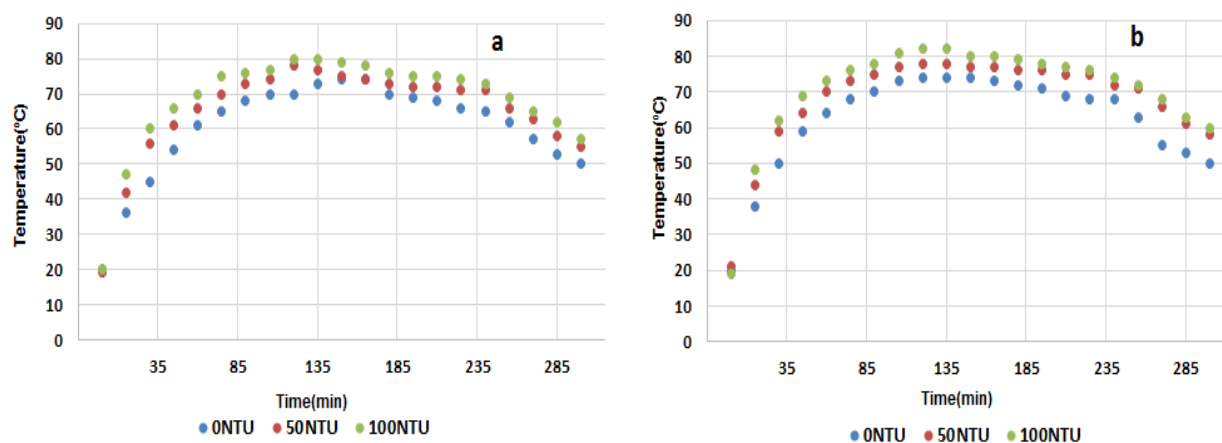


**Fig. 6.** Profiles of the average temperatures of the water recorded within the reactors CPC<sub>1</sub> (a), CPC<sub>2</sub> (b) containing water samples of different levels of turbidity.



However, considering the range of wavelengths of the sun's energy passes through the water, the absorption rate was low and the majority of the light passes through water [16]. In this research for the maximum use of the solar visible light, wavelength range of 300–1,600 nm, we used a black copper metal which was a strong absorbent of solar visible light. Kehoe *et al.* believe that the volume of used water can affect solar disinfection efficiency [44]. This issue can be investigated from two aspects: At first with increasing of water films, the solar disinfecting methods, the UV sun penetration and its effectiveness were reduced. Second, in the same conditions of sun exposure, when the mass of water increased, the rate of rising of water temperature reduced. In fact, based on equation (1), the rate of temperature increase was inversely related with the mass water. According to previous studies on CPCs using a concentrate factor in different volumes of water, disinfection was an important factor in increasing the volume level, when film depth contacting with UV increases, the efficiency of the disinfection reduced [45].

Turbidity was a limiting factor in the solar disinfection methods. One of the effects of turbidity created a shield for organisms, this shield in the direct contact with UV disinfection reduces efficiency [46]. In Table 1, the complete inactivation time of bacteria and the required energy in two different types of reactors are shown. As can be seen, the required times reaching the complete inactivation at the turbidity levels of 0, 50 and 100 NTU were 15, 45 and 60 min, respectively, for the CPC<sub>1</sub> and 30, 45 and 45 min, respectively for CPC<sub>2</sub> Fig. 5 (a, b). As shown in Table 1, the negative impacts of turbidity at the complete inactivation time of bacteria in the reactor CPC<sub>1</sub> were more significant ( $p < 0.0001$ ) than those in the other water samples in the reactor CPC<sub>2</sub> (0.05). Solar techniques were used to inactivate *E. coli* with increasing water turbidity from 5 to 50 and inactivation time from 150 min to 180 min [47]. However, with increasing turbidity in CPC from 5 to 100 NTU UV, the effect on oocyte inactivation was reduced but due to the increase of temperature caused by the absorption of sunlight, the effect turbidity significantly reduced [48]. In general, at the CPC<sub>2</sub> temperatures above 80 °C in addition to its synergistic effect with UV for water pasteurization, the effect of turbidity can be reduced, but at CPC<sub>1</sub> with increasing turbidity, light penetration is reduced significantly resulting in reduction of the effect nanocatalysts. Regrowth counts of bacteria were determined in all experiments. In none of the samples with certain conditions, there was no growth after cultivation.

Due to two simultaneous effects of high temperatures and UV, re-growth of solar disinfection was not seen in these examples.

#### 4. Conclusions

The use of CPC<sub>1</sub> with hydroxyl radicals (OH•) production significantly improved the efficiency of the old CPCS technique, since these systems (CPC<sub>1-2</sub>) shortened the exposure times to solar radiation and also minimized the negative effects of turbidity on the disinfected samples. This technology has been proved to be a good enhancement method to inactivate microorganisms under real conditions and represents a good alternative technique to drinking water treatment in developing countries.

#### References

- [1] J. Lonnen, S. Kilvington, S. Kehoe, F. Al-Touati, K. McGuigan, *Water. Res.* 39 (2005) 877-883.
- [2] E. Alonso, A. Santos, P. Riesco, *Fresenius Environ. Bulletin.* 14 (2005) 322-326.
- [3] S.C. Eleren, U. Alkan, A. Teksoy, *Fresenius Environ. Bulletin.* 23 (2014) 1397-1406.
- [4] A. Yazdanbakhsh, A. Rahmani, M. Massoudinejad, M. Jafari, M. Dashtdar, *Desalin. Water Treat.* 57 (2016) 23719-23727.
- [5] R. Khaengraeng, R. Reed, *J. Appl. Microbiol.* 99 (2005) 39-50.
- [6] P.M. Oates, P. Shanahan, M.F. Polz, *Water. Res.* 37 (2003) 47-54.
- [7] S. Malato, P. Fernández-Ibáñez, M. Maldonado, J. Blanco, W. Gernjak, *Catal. Today* 147 (2009) 1-59.
- [8] B. Khodadadi, *Iran. J. Catal.* 6 (2016) 305-311.
- [9] M. Pirhashemi, A. Habibi-Yangjeh, *Mater. Chem. Phys.* 214 (2018) 107-119.
- [10] H.R. Pouretdal, M. Fallahgar, F. Sotoudeh Pourhasan, M. Nasiri, *Iran. J. Catal.* 7 (2017) 317-326.
- [11] L. Shabani, H. Aliyan, *Iran. J. Catal.* 6 (2016) 221-228.
- [12] M. Pirhashemi, A. Habibi-Yangjeh, *Ceram. Inter.* 43 (2017) 13447-13460.
- [13] A. Besharati-Seidani, *Iran. J. Catal.* 6 (2016) 447-454.
- [14] J. Esmaili-Hafshejani, A. Nezamzadeh-Ejchieh, *J. Hazard. Mater.* 316 (2016) 194-203.
- [15] M.H. Fallah, *Iran. J. Catal.* 6 (2016) 281-292.
- [16] N. Ajoudanian, A. Nezamzadeh-Ejchieh, *Mater. Sci. Semi. Proc.* 36 (2015) 162-169.
- [17] A. Fujishima, T.N. Rao, D.A. Tryk, *J. Photochem. Photobiol. C* 1 (2000) 1-21.
- [18] C. Avşar, I. Berber, *Fresenius Environ. Bull.* 23 (2014) 2481-2487.
- [19] Y. Jiao, W. Ge, R. Qin, B. Sun, W. Jiang, D. Liu, *Fresenius Environ. Bull.* 21 (2012) 1375-1384.
- [20] D.M. Blake, P.C. Maness, Z. Huang, E.J. Wolfrum, J. Huang, W.A. Jacoby, *Sep. Purif. Methods* 28 (1999) 1-50.

- [21] Y. Abdollahi, A.H. Abdullah, Z. Zainal, N.A. Yusof, *Fresenius Environ. Bull.* 21 (2012) 256-262.
- [22] Z.-D. Meng, S.-B. Jo, L. Zhu, K. Ullah, S. Ye, W.-C. Oh, *Fresenius Environ. Bull.* 24 (2015) 481-491.
- [23] M. Tabatabaee, A. Ghotbifar, A.A. Mozafari, *Fresenius Environ. Bull.* 21 (2012) 1468-1473.
- [24] X. Zhang, K. Yan, D. Ren, H. Wang, *Fresenius Environ. Bull.* 16 (2007) 632-638.
- [25] M. Ahmadi, K. Rahmani, A. Rahmani, H. Rahmani, *Pol. J. Chem. Technol.* 19 (2017) 104-112.
- [26] M. Farzadkia, K. Rahmani, M. Gholami, A. Esrafil, A. Rahmani, H. Rahmani, *Korean. J. Chem. Eng.* 31 (2014) 2014-2019.
- [27] M. Gholami, K. Rahmani, A. Rahmani, H. Rahmani, A. Esrafil, *Desalin. Water Treat.* 57 (2016) 13878-13886.
- [28] K. Sunada, T. Watanabe, K. Hashimoto, *J. Photochem. Photobiol. A* 156 (2003) 227-233.
- [29] K. Sivagami, R.R. Krishna, T. Swaminathan, *Sol. Energy* 103 (2014) 488-493.
- [30] M. Chaudhuri, H. Zuhali, A.C. Affam, *Int. J. Photoenergy* 2013 (2013) Article ID 435017.
- [31] C. Shifu, C. Gengyu, *Sol. Energy*. 79 (2005) 1-9.
- [32] K. Sivagami, R. Ravi Krishna, T. Swaminathan. *Sol. Energy*. 103 (2014) 488-493.
- [33] J.-J. Feng, Q.-C. Liao, A.-J. Wang, J.-R. Chen, *CrystEngComm* 13 (2011) 4202-4210.
- [34] R.K. Oshiro, *Method 1604: Total Coliforms and Escherichia coli in Water by Membrane Filtration Using a Simultaneous Detection Technique (MI Medium)*, Environmental Protection Agency, Washington D.C., 2002.
- [35] H. Derikvandi, A. Nezamzadeh-Ejehieh, *J. Mol. Catal. A: Chem.* 426 (2017) 158-169.
- [36] S. Aghabeygi, R. Kia Koojori, H. Vakili Azad, *Iran. J. Catal.* 6 (2016) 275-279.
- [37] M. Babaahamdi-Milani, A. Nezamzadeh-Ejehieh, *J. Hazard. Mater.* 318 (2016) 291-301.
- [38] L.S. Roselin, R. Selvin, *Sci. Adv. Mater.* 3 (2011) 251-258.
- [39] B. Khodadadi, M. Bordbar, *Iran. J. Catal.* 6 (2016) 37-42.
- [40] A. Nezamzadeh-Ejehieh, M. Bahrami, *Desalin. Water Treat.* 55 (2015) 1096-1104.
- [41] M. Pirhashemi, A. Habibi-Yangjeh, *Sep. Purif. Technol.* 193 (2018) 69-80.
- [42] K. McGuigan, T. Joyce, R. Conroy, J. Gillespie, M. Elmore-Meegan, *J. Appl. Microbiol.* 84 (1998) 1138-1148.
- [43] B. Sommer, A. Marino, Y. Solarte, M. Salas, C. Dierolf, C. Valiente, D. Mora, R. Rechsteiner, P. Setter, W. Wirojanagud, *Aqua* 46 (1997) 127-137.
- [44] S. Kehoe, T. Joyce, P. Ibrahim, J. Gillespie, R. Shahar, K. McGuigan, *Water Res.* 35 (2001) 1061-1065.
- [45] M. Fontán-Sainz, H. Gómez-Couso, P. Fernández-Ibáñez, E. Ares-Mazás, *Am. J. Trop. Med. Hyg.* 86 (2012) 223-228.
- [46] H. Gómez-Couso, M. Fontán-Sainz, K.G. McGuigan, E. Ares-Mazás, *Acta Trop.* 112 (2009) 43-48.
- [47] H. Gómez-Couso, M. Fontán-Sainz, C. Sichel, P. Fernández-Ibáñez, E. Ares-Mazás, *Trop. Med. Int. Health* 14 (2009) 620-627.
- [48] H. Gómez-Couso, M. Fontán-Sainz, E. Ares-Mazás, *Am. J. Trop. Med. Hyg.* 82 (2010) 35-39.